ISSN 1819-7140, Russian Journal of Pacific Geology, 2017, Vol. 11, No. 5, pp. 339–353. © Pleiades Publishing, Ltd., 2017.
Original Russian Text © V.A. Rashidov, O.V. Pilipenko, V.V. Petrova, 2017, published in Tikhookeanskaya Geologiya, 2017, Vol. 36, No. 5, pp. 29–43.

# Specific Features of the Mineral Composition and Petromagnetic Properties of Rocks from the Minami-Khiosi Submarine Volcano (Mariana Island Arc)

**V. A. Rashidov[a], *, O. V. Pilipenko[b], and V. V. Petrova[c]**

[a] *Institute of Volcanology and Seismology, Far East Branch of Russian Academy of Sciences, bulv. Piipa 9, Petropavlovsk-Kamchatsky, 683006 Russia*

[b] *Schmidt Institute of Physics of the Earth of the Russian Academy of Sciences, ul. Bol'shaya Gruzinskaya 10-1, Moscow, 123995 Russia*

[c] *Geological Institute, Russian Academy of Sciences, Pyzhevskii per. 7, Moscow, 119017 Russia*

**e-mail: rashidva@kscnet.ru*

Received February 26, 2016

**Abstract**—Complex studies of the mineral composition and petromagnetic properties of the rocks which compose an edifice of the Minami–Khiosi submarine volcano located in the Mariana island arc are carried out for the first time. The Minami–Khiosi Volcano is a part of the Khiosi volcanic complex within the alkaline province of the Idzu–Bonin and Mariana island arcs. All of the rocks analyzed are enriched in $K_2O$ (1.34–3.30%), Ba (370–806 ppm), and Sr (204–748 ppm). The basalt has a porhyric texture and contains mosTy olivine phenocrysts as individual crystals and growths with a size up to 2 cm; the groundmass is fine-crystalline. The samples studied contain at least three Fe-bearing oxide minerals. These are predominant magnetite and less abundant ilmenite and Fe hydroxides. It is established that the samples studied are magnetically isotropic and have high values of natural remanent magnetization and Königsberger ratio. Similarly to the other island-arc Late Cenozoic submarine volcanoes in the western part of the Pacific Ocean, the samples studied are strongly differentiated by the value of natural remanent magnetization and magnetic susceptibility. The low-coercivity magnetic minerals (titanomagnetite and magnetite) of the pseudo-single-domain structure, as well as high-coercivity minerals (hematite) are the main carriers of magnetization. The high values of natural remanent magnetization are explained by the pseudo-single-domain structure of the titanomagnetite grains, whereas the high values of magnetic susceptibility result from the high concentration of ferromagnetic grains.

**Keywords:** basalt, mineralogical and petromagnetic studies, submarine volcano, Minami–Khiosi, Mariana island arc

**DOI:** 10.1134/S1819714017050049

## INTRODUCTION

Comparative analysis of the magnetic properties of the rocks which compose the submarine volcanoes of the Kuril, Idzu–Bonin, Mariana, and Solomon island arc of the Pacific transitional zone performed by the authors [2, 3, 7, 8, 12–15] shows that they are strongly differentiated by the value of natural remanent magnetization and magnetic susceptibility. The samples are magnetically isotropic and contain relatively low-coercivity magnetic minerals. The grains of unaltered and/or oxidized titanomagnetite of the different domain structure are the main carriers of magnetization in the rocks studied. The high values of natural remanent magnetization in the rock samples studied are explained by the pseudo-single-domain structure of the titanomagnetite grains, whereas the high values of magnetic susceptibility result from the high content of ferromagnetic grains.

In this paper, we report the results of investigation of the peculiarities of the material composition and petromagnetic properties of the rocks which compose an edifice of the Minami–Khiosi active submarine volcano located in the Mariana island arc.

The Mariana island arc is a classical young island arc in the western part of the Pacific Ocean. Most of islands and submarine volcanoes in its northern part were formed in the Late Pliocene. The southern part of the arc is older: the volcanoes are of Eocene–Miocene age [1]. There are nine active continental volcanoes and 63 submarine volcanoes in the Mariana arc; nine of the submarine volcanoes may be currenTy considered as active [3, 4, 9–11, 16, 17, 19, 34].

The Minami–Khiosi Volcano (South Minami, Minami–Khiosi–Kaisan) of Quaternary age is one such active submarine volcano [43]. Its volcanic activity has been registered repeatedly starting from August 25, 1975 [10, 11, 29, 34]. The Minami–Khiosi submarine volcano is a part of the Khiosi volcanic complex within the alkaline province of the Idzu–Bonin and Mariana island arcs [28, 37–39]. This volcano was studied during the 5th, 10th, and 13th voyages of R/V "Vulkanolog" in 1978, 1981, and 1982; in voyage TT-192 of R/V "Thomas G. Thompson" of Washington University in 1985 [16, 17]; and in voyages of the geological and hydrographical surveys of Japan [5, 22, 29, 40–42].

The Minami–Khiosi submarine volcano (Figs. 1 and 2) spreads from the depth of 1500 m, where its size is ~20 × 15 km. The near-top part of the edifice limited with an isobath of 200 m has a size of 1.8 × 0.6 km and is elongated in the northwestern direction. The steepness of the slopes is 8°–9° in the range of 1500–1000 m; 5.5°–18.5° in the range of 1000°–500°; and 9°–24° in the range of 500–100 m.

The minimal depth above the top of the volcano registered in the 5th voyage of R/V "Vulkanolog" is 100 m. The minimal depth of ~100 m is evident from the data of [33], 96 m from the data of [35, 36], and 30 m from [43].

The volume of the volcanic edifice is estimated as ~95 $km^3$ [10]; according to the data of [16], the volume of the volcano is 109 $km^3$.

A rise with active fumaroles was revealed at a depth of 100–120 m in the 10th voyage of R/V "Vulkanolog" (Fig. 3). The Minami–Khiosi submarine volcano is clearly reflected in the potential fields by local anomalies from its edifice [5, 10, 11, 22, 23, 27, 40, 41]. A positive anomaly with an intensity of 158 mGal is confined to the volcanic edifice on the gravimetric map in free air reduction [5, 22].

The intensity of the magnetic anomaly $\Delta T_a$ of the Minami–Khiosi submarine volcano is 3000 nT [10, 11, 22, 23, 30]. The magnetic anomaly is produced by a body with a volume of 0.17 $km^3$ and located in the near-top part of the edifice in a depth range of 150–600 m [10, 11]. Most likely, this body is a lava plug.

In this paper, we attempt to find relationships between the mineral composition of rocks dredged from the Minami–Khiosi edifice and their petromagnetic characteristics using modern methods and apparatus.

## METHODS OF THE STUDY

The microprobe analysis of ore minerals was carried out at the Geological Institute of Russian Academy of Sciences, on a Cam Scan MV2300 analytical scanning electron microscope (analysts N.V. Gor'kova and A.T. Savichev) and at the Russian Institute of Mineral Resources on a JXA-8100 microprobe (JEOL) equipped with an INCA energy-dispersive spectrometer (analyst I.G. Bystrov). The composition of the central zones revealed upon polishing and on unpolished surface parts of manually selected grains was analyzed in Fe-bearing and associated minerals from all samples. Since the valence of iron cannot be recognized during the microprobe analysis, the standard ratio (2/3 of trivalent iron and 1/3 of divalent iron) was taken in all cases for recalculation of the average compositions of titanomagnetite for the mineral formula. The conversion coefficient for the transition of $Fe^{2+}$ to $Fe^{3+}$ was accounted as well.

Petromagnetic studies were performed at the Laboratory of the Main Geomagnetic Field and Petromagnetism, Schmidt Institute of Physics of the Earth of the Russian Academy of Sciences. The natural remanent magnetization (Jn) of the samples was measured on a JR-6 magnetometer (AGICO, Czech Republic) in three orthogonal positions of sample rotation. The magnetic susceptibility ($\chi$) and degree (P') of anisotropy of magnetic susceptibility (AMS) were measured on a Multi-Function Kappabridge kappameter (AGICO, Czech Republic). The stability of Jn in relation to the influence of an alternating magnetic field, i.e., the median magnetic field, was studied in all samples. This was performed by the study of the complete curves of demagnetization by an alternating magnetic field up to a maximum value of 100 mT with a step of 5 mT. Processing with an alternating magnetic field was carried out on an instrument built in a cryogenic (SQUID) magnetometer (2G Enterprises, United States), which was located in a nonmagnetic room produced by Lodestar Magnetics (United States) decreasing the outer magnetic field by a factor of >200.

The curves of magnetic hysteresis were obtained on a vibromagnetometer (ORION, Russian Federation), which allowed us to estimate the domain state [18, 19].

The composition of the magnetic fraction was studied using the curves of saturation remanent magnetization (Jrs) produced in an ASC IM-100 impulse magnetizing apparatus (2G Enterprises, United States) in a constant magnetic field from 0 to 0.8 T, as well as by measurement of the remanent coercivity force Bcr. Thermomagnetic analysis (TMA) was performed on a Multi-Function Kappabridge kappameter (AGICO, Czech Republic) using the dependence of the mass magnetic susceptibility on temperature $k(T)$ for powder samples with a weight of ~1 g. The TMA by $k(T)$ is a rapid and very sensitive method for analysis of magnetic phases and the composition of titanomagnetite [24]. With account for the recommendations of [32], in this study, the magnetic phases were determined by the Hopkinson peaks (if present) near the Currier points on the $k$(T) curves, on the basis of the Currier–Weiss law; if there were no peaks, the magnetic phases were determined by the method of two tangents [21].

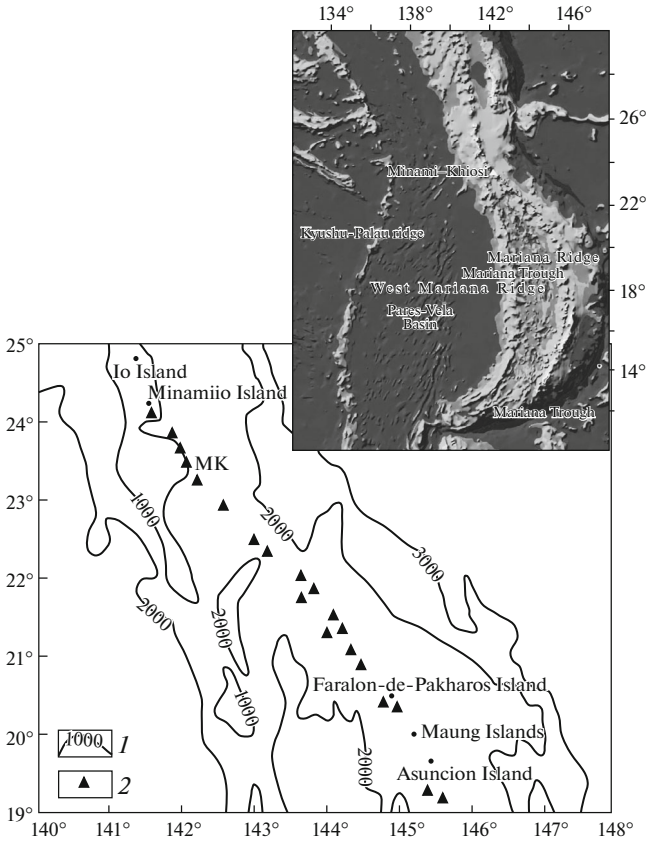


**Fig. 1.** Location of the Minami–Khiosi submarine volcano. (*1*) Isobaths; (*2*) submarine volcanoes. MK, Minami–Khiosi.

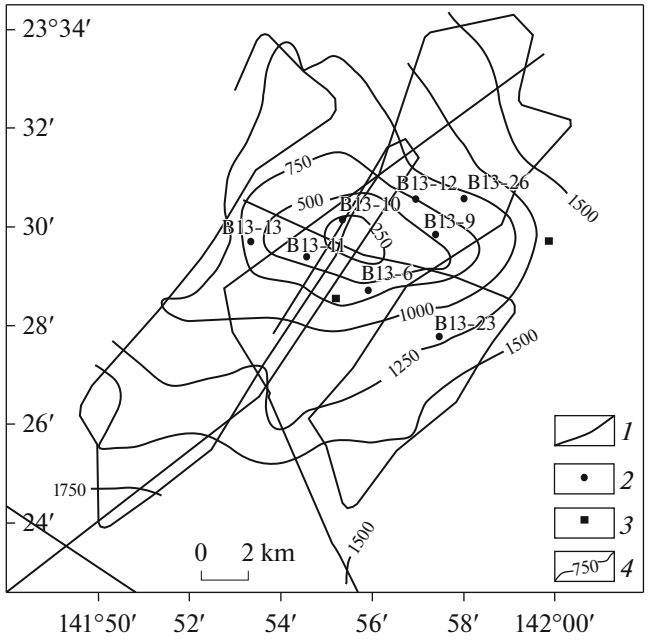


**Fig. 2.** Bathymetric scheme of the Minami–Khiosi submarine volcano. (*1*) Tacks; (*2*, *3*) stations of dredging in the 5th voyage of R/V "Vulkanolog" and in voyage TT-192 of R/V "Thomas G. Thompson"; (*4*) isobaths (m).

## MINERAL COMPOSITION OF ROCKS

The Minami–Khiosi Volcano edifice was dredged twice during voyage TT-192 of R/V "Thomas G. Thompson" (Fig. 2) and plagioclase–olivine–clinopyroxene basalt and andesite–basalt were collected [16, 17]. Studying the dredged rocks, Blumer et al. [16, 17, 25] established the alkaline character of the rocks from the Minami–Khiosi Volcano and noted the similarity of their compositions with shoshonite. They suggested that such rocks could have formed only under specific tectonic conditions with access to the deep enriched parts of the manTe, such as subduction zones and zones of back-arc spreading or deep volcanism.

In the 5th voyage of R/V "Vulkanolog", the volcano was dredged eight times from the slopes and near-top part (Fig. 2). The dredged rocks (Table 1) were represented by a genetically related group of basalt with different contents of phenocrysts and various degrees of groundmass crystallization.

Porous slag predominated among the dredged rocks. The most unaltered slag was collected from the near-top part of the volcano and most likely was related to the near-vent facies. The samples subjected to the influence of high-temperature fumaroles were dredged from the same place; among them are strongly altered basalt and fragments of native sulfur with a diameter of 1–2 cm. There are sulfur fragments with ash impurity. Crusts of lava flows and massive glassy basalt were collected upon dredging of the volcanic edifice as well. The typical distribution of volcanogenic–sedimentary rocks with depth was registered. Down the slope, lithified slag is replaced with tufogenic polymictic sandstone, gritstone, and aleurite [10].

The textures of the rocks from the Minami–Khiosi Volcano, the distribution of iron minerals in them, and the chemical composition of the dredged rocks are reported in Figs. 4 and 5 and in Table 2.

All of the rocks analyzed are enriched in $K_2O$ (1.34–3.30%), have high total alkalinity (4.7–7.3%), and are characterized by high concentrations of P (0.44–0.81), Rb (16–68 ppm, mainly 30–50 ppm), Ba (370–806 ppm), Sr (479–789 ppm, mainly 524–700 ppm), and Zr (mainly 107–225 ppm) (Table 2). $K_2O/Na_2O$ ranges from 0.38 to 0.92 [14]. These values are in a good agreement with the previously published data [16, 17, 25, 26, 28, 31, 39]. The chemical composition of the rocks is characterized by a quite high concentration of $TiO_2$ (1.94–2.81%) and its homogeneous distribution in different flows, as well as by the negative correlation in the concentrations of $Fe^{2+}$ and $Fe^{3+}$. Attention is drawn to the almost positive correlation between the concentrations of $Al_2O_3$, FeO, and CaO.

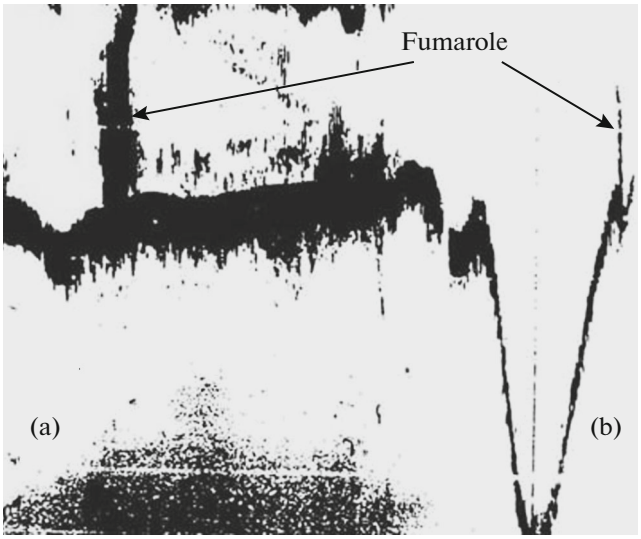


**Fig. 3.** Fragments of echo sounding profiles performed in the 10th voyage of R/V "Vulkanolog" illustrating the fumarole activity of the Minami–Khiosi submarine volcano. (a) In the drift; (b) on the way of R/V. Echo sounder WD-110M (operating frequency of 12.5 kHz).

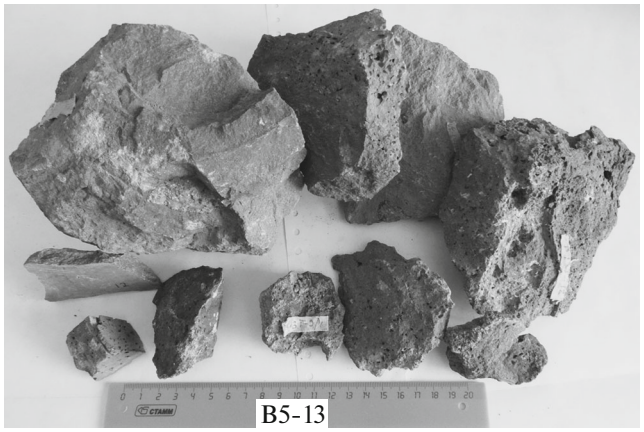


**Fig. 4.** Samples of dredged rocks. Light (brownish-yellow) spots in the gray matrix are the glomeroporphyry aggregates of olivine crystals.

Our analytical studies and literature data show that the volcanic rocks composing the Minami–Khiosi submarine volcano relate to the alkaline formations.

Basalt has a porphyric texture. The composition, size, and content of the phenocrysts vary between flows. The texture of the groundmass is usually doleritic with the mineral content of glass. The rock is porous and the pores are sometimes filled with organic material, presumably bitumen.

The phenocrysts are mosTy represented by olivine as individual crystals or their aggregates. The size of the olivine in some samples may be very large (up to 2 cm), whereas the groundmass is fine crystalline (Fig. 4). Intergrowths of olivine phenocrysts with smaller clinopyroxene (pigonite) crystals and olivines

**Table 1.** Dredged samples of rocks composing the edifice of the Minami–Khiosi submarine volcano

| Sample | Rock |
|---|---|
| B-5-13-6 | Coarse-porphyry basalt. Groundmass is fine-crystalline, content of noncrystallized glass is low |
| B-5-13-9 | Aphyric basalt, the texture of groundmass is from fine- to medium-granular, glass is almost completely crystallized, rare pores are observed |
| B-5-13-9/1<br>B-5-13-9/2 | Analogs of Sample B-5-13-9, but in some areas porphyry, small content of olivine phenocrysts and glomeroporphyry intergrowths are observed |
| B-5-13-10/2 | Medium-crystalline aphyric basalt, but sometimes individual phenocrysts of olivine replaced with iddingsite are observed. Glass is almost completely crystallized. The rock contains up to 10% of unfilled pores (gas pores) |
| B-5-13-12/1<br>B-5-13-12/2 | Analogs of Sample B-5-13-10/2, but the content of olivine and the degree of its alteration are sligh Ty higher |
| B-5-13-12/3 | Crystallolithovitroclastic tuff cemented with carbonate. All components of tuff have basic (basaltic) composition |
| B-5-13-12/4 | Basalt with minor phenocrysts, carbonated in some places |
| B-5-13-13 | Crystallolithovitroclastic tuff cemented with carbonate. All components of tuff have basic (basaltic) composition |
| B-5-13-23 | Basalt with minor phenocrysts, groundmass is from medium- to coarse-crystalline, poorly porous |
| B-5-13-26/1 | Crystallolithovitroclastic basaltic with carbonate, partially clayey–chlorite cement. Glass of fragments has large pores |
| B-5-13-sh | Porous basaltic glass with a small content of plagioclase |

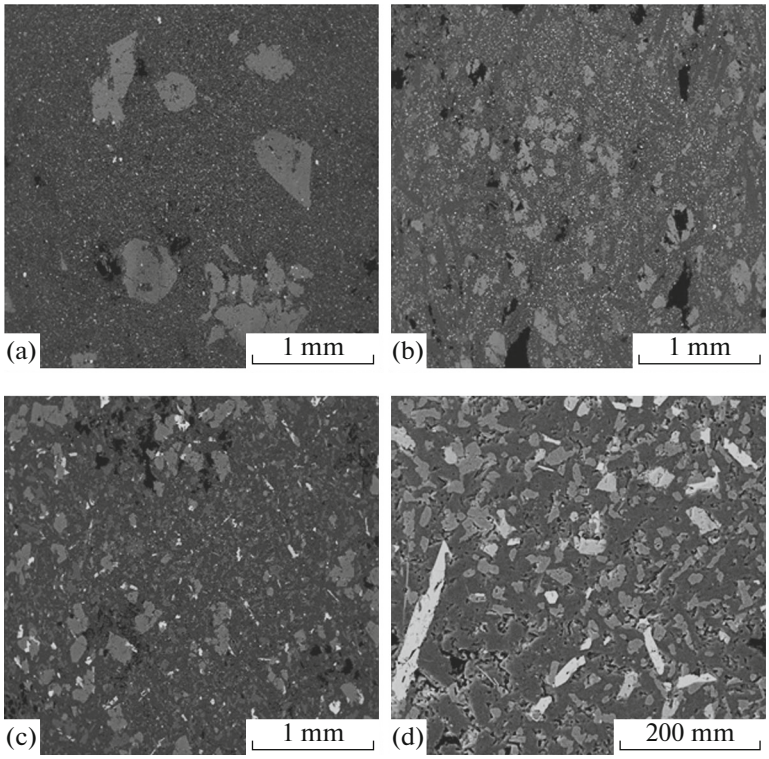


**Fig. 5.** Textures of lavas from the Minami–Khiosi Volcano and distribution of Fe minerals in rocks. (a) Sample B-5-13-6, olivine megacrysts (light gray) clearly observed against the background of cryptocrystalline groundmass of rock. White spots in the groundmass are titanomagnetite microlites; (b) Sample B-5-13-9, phenocrysts of pyroxene (light gray) and plagioclase (dark gray elongated laths in the fine-crystalline groundmass of the rock). White spots in the groundmass are titanomagnetite microlites; (c) Sample B-5-13-12/1, phenocrysts of olivine, pyroxene (gray with different shades), and plagioclase (dark gray, almost black laths) against the background of fine-crystalline groundmass of rock. White elongated rectangles are ilmenite crystals; white isometric crystals are represented by titanomagnetite. Crystals of ore minerals sometimes reach the size of phenocrysts; (d) Sample B-5-13-23, groundmass of dolerite consisting of microlites of pyroxene (gray), plagioclase (dark-gray, almost black), and segregations of ilmenite (white elongated crystals) and titanomagnetite (light gray and white pseudo-isometric grains). Black shapeless spots in all photographs are unfilled pores in the rocks.

with small titanomagnetite and chrome spinel crystals are occasional. The theoretical composition of the pigonite is (Mg, Fe, Ca)(Mg, Fe)$Si_2O_6$. The concentration of Ca ranges within 0.13–0.28 formula units (hereinafter, f.u.), the content of Al does not exceed 2 wt %, and the content of Mn is high. Among the mineralogical formulae reported, this is fulfilled in two points of three:

Sample B-5-13-6, point 11:
$(Mg_{1.15}Fe_{0.65}Ca_{0.19}Mn_{0.01})_{2.00}(Si_{1.95}Al_{0.01}Ti_{0.01})_{1.97}O_{6.00}$;
Sample B-5-13-6, point 5:
$(Mg_{1.20}Fe_{0.64}Ca_{0.18}Mn_{0.01})_{2.03}(Si_{1.94}Fe_{0.03}Al_{0.02}Ti_{0.01})_{2.00}O_{6.00}$;
Sample B-5-13-6, point 2:
$(Mg_{0.98}Fe_{0.70}Ca_{0.14}Mn_{0.01})_{1.88}Si_{2.05}O_{6.00}$.

In a few samples, phenocrysts are represented by clinopyroxene (augite) and plagioclase (labradorite), as well as ore minerals (titanomagnetite and ilmenite), but their size is much smaller than that of olivine. The groundmass consists of the above-mentioned minerals almost in equal proportions. Among the accessory minerals are pyrite and chalcopyrite. The late minerals include Fe hydroxides, siderite, quartz, gypsum, and anhydrite. A detailed description of the nonmetallic minerals will be given in a special publication.

The tuffogene rocks (Samples B-5-13-13 and B-5-13-26/1) are represented by crystallolithovitroclastic tuff cemented with carbonate. The crystalline part includes fragments of quartz, pyroxene, and a small portion of olivine. The lithoclastic part comprises dolerite fragments and poorly crystallized glass with pla-

**Table 2.** Chemical composition of dredged samples of rocks composing an edifice of the Minami–Khiosi submarine volcano

| Rock | Basalt | | | | | | | | | Tuff | Basalt | Tuff | Slag |
|---|---|---|---|---|---|---|---|---|---|---|---|---|---|
| Sample | B-5-13-6 | B-5-13-9 | B-5-13-9/1 | B-5-13-9/2 | B-5-13-10/2 | B-5-13-12/1 | B-5-13-12/2 | B-5-13-12/3 | B-5-13-12/4 | B-5-13-13 | B-5-13-23 | B-5-13-26/1 | B-5-13-sh |
| Concentration, wt % | | | | | | | | | | | | | |
| $SiO_2$ | 52.87 | 51.53 | 52.30 | 51.24 | 52.82 | 48.09 | 50.62 | 53.88 | 49.70 | 56.68 | 53.38 | 52.06 | 53.45 |
| $TiO_2$ | 1.95 | 2.73 | 2.60 | 2.81 | 2.12 | 2.25 | 2.32 | 2.41 | 2.42 | 2.19 | 1.98 | 2.30 | 1.11 |
| $Al_2O_3$ | 13.61 | 12.63 | 13.49 | 12.57 | 14.14 | 12.89 | 13.50 | 12.77 | 13.37 | 9.51 | 14.25 | 10.23 | 17.37 |
| $Fe_2O_3$ | 4.96 | 5.14 | 2.62 | 5.05 | 3.69 | 3.13 | 4.49 | 8.66 | 2.43 | 7.65 | 3.07 | 5.93 | 10.45 |
| FeO | 6.40 | 6.49 | 7.89 | 6.71 | 6.36 | 7.22 | 6.59 | 2.32 | 7.65 | 1.01 | 7.56 | 2.32 | |
| MnO | 0.14 | 0.16 | 0.16 | 0.16 | 0.16 | 0.16 | 0.17 | 0.18 | 0.16 | 0.12 | 0.16 | 0.12 | 0.18 |
| MgO | 5.36 | 5.41 | 4.94 | 5.66 | 4.78 | 8.11 | 5.81 | 3.49 | 6.05 | 4.38 | 5.08 | 5.27 | 3.00 |
| CaO | 8.23 | 7.99 | 7.90 | 8.32 | 8.43 | 9.06 | 8.67 | 6.53 | 9.17 | 3.66 | 8.30 | 7.37 | 8.91 |
| $Na_2O$ | 3.35 | 3.77 | 3.58 | 3.66 | 3.97 | 3.07 | 3.51 | 4.00 | 3.57 | 1.96 | 3.60 | 1.78 | 3.23 |
| $K_2O$ | 1.34 | 2.09 | 2.84 | 2.14 | 1.98 | 2.32 | 2.50 | 3.30 | 2.57 | 1.60 | 1.37 | 1.65 | 1.79 |
| $P_2O_5$ | 0.44 | 0.67 | 0.81 | 0.66 | 0.62 | 0.61 | 0.67 | 0.77 | 0.67 | 0.36 | 0.39 | 0.42 | 0.19 |
| L.O.I. | 0.64 | 0.68 | <0.1 | 0.28 | 0.22 | 2.30 | 0.44 | 1.43 | 1.40 | 10.77 | <0.1 | 10.30 | 0.33 |
| Total | 99.29 | 99.28 | 99.12 | 99.26 | 99.28 | 99.20 | 99.29 | 99.74 | 99.15 | 99.89 | 99.15 | 99.74 | 100.01 |
| S | 0.03 | 0.08 | 0.07 | 0.19 | 0.19 | 1.31 | 0.23 | 0.10 | 1.15 | 0.18 | 0.05 | 0.19 | 0.19 |
| Concentration, ppm | | | | | | | | | | | | | |
| Cu | 56 | 39 | 57 | 47 | 61 | 51 | 57 | 42 | 46 | 38 | 69 | 37 | 200 |
| Zn | 131 | 219 | 129 | 221 | 127 | 166 | 111 | 187 | 110 | 95 | 120 | 99 | 95 |
| As | 7.4 | 4.5 | <2.0 | <2.0 | <2.0 | <2.0 | 3.6 | <2.0 | 3.6 | <2.0 | <2.0 | 5.7 | – |
| Pb | 5.1 | 5.1 | 6.1 | 8.9 | 7.7 | 4.4 | 3.9 | 7.8 | 8.3 | 8.1 | 5.8 | 9.8 | 12 |
| Co | 43 | 46 | 50 | 48 | 44 | 51 | 52 | 47 | 45 | 38 | 42 | 33 | <5 |
| Ni | 249 | 239 | 232 | 222 | 179 | 287 | 221 | 172 | 186 | 206 | 212 | 175 | 20 |
| Ga | 19 | 20 | 22 | 20 | 20 | 18 | 20 | 23 | 19 | 15 | 20 | 15 | 15 |
| Rb | 27 | 16 | 50 | 30 | 35 | 42 | 46 | 68 | 45 | 37 | 24 | 48 | 48 |
| Sr | 524 | 704 | 684 | 728 | 557 | 748 | 720 | 789 | 771 | 204 | 479 | 419 | 580 |
| Y | 27 | 29 | 28 | 28 | 27 | 24 | 24 | 28 | 24 | 25 | 25 | 24 | 25 |
| Zr | 139 | 211 | 225 | 197 | 199 | 204 | 215 | 307 | 213 | 202 | 142 | 203 | 160 |
| Nb | 25 | 41 | 43 | 39 | 34 | 40 | 42 | 55 | 42 | 37 | 24 | 37 | 9 |
| Mo | 4.7 | 2.4 | 1.5 | 5.0 | 2.5 | 1.8 | 3.0 | 2.9 | 2.0 | 2.2 | 2.8 | 3.1 | 4 |
| Ba | 370 | 527 | 640 | 595 | 442 | 638 | 727 | 806 | 636 | 470 | 403 | 613 | 650 |
| Th | 3.6 | 5.7 | 7.2 | 5.4 | 5.2 | 6.3 | 6.5 | 8.8 | 7.3 | 7.9 | 5.1 | 9.7 | 14 |
| U | <2.0 | 2.1 | <2.0 | 2.1 | <2.0 | 3.8 | <2.0 | <2.0 | 2.0 | <2.0 | <2.0 | <2.0 | 3 |

Sample B-5-13-sh contains (%) Cl (0.12) and F (0.04).

**Table 3.** Average compositions of titanomagnetites and ilmenites from the Minami–Khiosi submarine volcano (wt %)

| Mineral | Titanomagnetite | | | | Data from [16] | Ilmenite | | | |
|---|---|---|---|---|---|---|---|---|---|
| sample | B-5-13-6 | B-5-13-9 | B-5-13-12/1 | B-5-13-23 | | B-5-13-6 | B-5-13-9 | B-5-13-12/1 | B-5-13-23 |
| average analysis | 3 | 4 | 7 | 2 | | 7 | 7 | 4 | 17 |
| Si | 0.00 | 0.00 | 0.00 | 0.00 | 0.1 | 1.82 | 0.06 | 0.23 | 0.49 |
| Ti | 9.29 | 6.50 | 14.63 | 8.40 | 5.37 | 27.02 | 29.25 | 29.88 | 30.21 |
| Al | 1.25 | 2.06 | 0.71 | 0.00 | 2.84 | 0.89 | 0.11 | 0.00 | 0.08 |
| $Fe^{2+}$ | 18.02 | 19.93 | 17.22 | 22.28 | 20.66 | 33.52 | 33.96 | 33.79 | 35.12 |
| $Fe^{3+}$ | 39.86 | 43.84 | 37.89 | 44.56 | 41.33 | | | | |
| Mn | 0.24 | 0.14 | 0.43 | 0.00 | 0.53 | 0.20 | 0.50 | 0.45 | 0.04 |
| Mg | 1.34 | 1.58 | 1.64 | 0.00 | 1.40 | 2.36 | 2.71 | 2.50 | 1.14 |
| Ca | 0.00 | 0.00 | 0.00 | 0.00 | 0.10 | 0.62 | 0.10 | 0.04 | 0.07 |
| Na | 0.00 | 0.00 | 0.00 | 0.00 | 0.00 | 0.30 | 0.00 | 0.00 | 0.00 |
| V | 0.39 | 0.42 | 0.42 | 0.00 | 0.00 | 0.11 | 0.19 | 0.17 | 0.37 |
| Cr | 3.77 | 0.22 | 0.14 | 0.00 | 0.00 | 0.43 | 0.07 | 0.00 | 0.00 |
| 0 | 25.81 | 25.62 | 26.94 | 24.76 | 23.63 | 32.81 | 32.21 | 31.82 | 31.94 |
| Total | 99.96 | 100.31 | 100.02 | 100.00 | 95.76 | 100.07 | 99.16 | 98.86 | 99.47 |

All Fe is given as $Fe^{2+}$ for ilmenite. Analysis from [16] contains K (0.04 wt %).

gioclase. Pumice-like glass with pores partially filled with bitumen, carbonate, and presumably zeolites predominates.

The slag (Sample B-5-13-sh) is composed of expanded gas-saturated glass, poorly crystallized with plagioclase. The gas pores are sometimes filled with bitumen. Orange crusts of quenching (probably palagonite) occur in the marginal zones of the glass. Ore minerals are absent.

Each sample studied, except for the slag, contains at least three Fe-bearing minerals. These are predominant magnetite and smaller contents of ilmenite and Fe hydroxides.

In addition to Fe and Ti, almost all of the samples of titanomagnetite (theoretical composition $Fe^{2+}(FeTi^{3+})_2O_4$) contain small portions of Mg, Al, and V (Table 3).

Calculation of the analyses given in Table 3 provides the following crystallochemical formulae of titanomagnetite:

Sample B-5-13-6:

$(Fe^{2+}_{0.63}Mg_{0.11}Mn_{0.01})_{0.75}(Fe^{3+}_{1.40}Ti_{0.38}Al_{0.09}V_{0.01}Cr_{0.14})_{2.02}O_4$;

Sample B-5-13-9:

$(Fe^{2+}_{0.71}Mg_{0.13})_{0.84}(Fe^{3+}_{1.56}Ti_{0.27}Al_{0.15}V_{0.02}Cr_{0.01})_{2.01}O_4$;

Sample B-5-13-12/1:

$(Fe^{2+}_{0.59}Mg_{0.13}Mn_{0.01})_{0.73}(Fe^{3+}_{1.31}Ti_{0.59}Al_{0.05}V_{0.01})_{1.96}O_4$;

Sample B-5-13-23:

$(Fe^{2+}_{0.82})_{0.82}(Fe^{3+}_{1.64}Ti_{0.36})_{2.00}O_{4.00}$.

Each formula is characterized by a lack of divalent cations. The content of Ti per elementary cell of titanomagnetite is the following: Sample B-5-13-6, 0.38; Sample B-5-13-9, 0.27; Sample B-5-13-12/1, 0.59; Sample B-5-13-23, 0.36 f. u.

Ilmenite with the theoretical composition $(FeTi)_2O_3$ always contains impurities of Si and Ca and rarely of Na, V, and Cr (Table 3). Calculation of the chemical compositions provides the following crystallochemical formulae of ilmenite:

Sample B-5-13-6, $(Fe_{0.90}Ti_{0.85}Mg_{0.15}Si_{0.07}Al_{0.05}Ca_{0.02}Na_{0.02}Cr_{0.01})_{2.02}O_3$;

Sample B-5-13-9:

$(Ti_{0.90}Fe_{0.87}Mg_{0.26}Mn_{0.02}Al_{0.01})_{2.06}O_3$;

Sample B-5-13-9/1:

$(Fe_{0.95}Ti_{0.94}Mg_{0.13}Mn_{0.01}V_{0.01})_{2.04}O_3$;

Sample B-5-13-12:

$(Ti_{0.92}Fe_{0.89}Mg_{0.19}Mn_{0.02}Si_{0.01})_{2.03}O_3$;

Sample B-5-13-23:

$(Fe_{0.95}Ti_{0.95}Mg_{0.07}Si_{0.03}V_{0.01})_{2.01}O_3$.

The minimum concentrations of Fe and Ti in the ilmenite are 25.4 and 29.7 wt %, respectively; the maximum concentration of Fe and Ti are 33.8 and 38.4 wt %, respectively (0.85–0.95 f.u. Ti, 0.87–0.95 f.u. Fe).

However, we may conclude that any sample contains almost equal concentrations of Ti and Fe (f.u.): 0.80 Ti and 0.85 Fe in Sample B-5-13-6; 0.86 Ti and

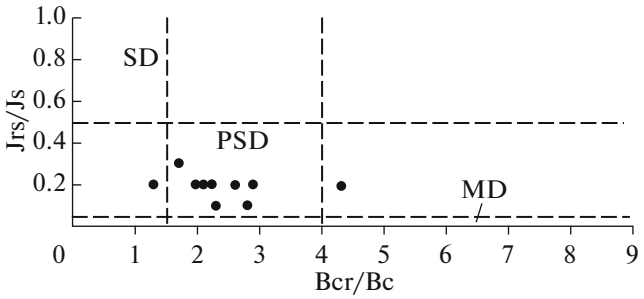


**Fig. 6.** Day diagram.

0.83 Fe in Sample B-5-13-9; 0.86 Ti and 0.83 Fe in Sample B-5-13-12; and 0.95 Ti and 0.95 Fe in Sample B-5-13-23.

There are small contents of iron oxides and hydroxides (hematite, limonite, etc.) in all samples. Since they partially replace primary minerals, mosTy olivine, their content and composition are very irregular.

## PETROMAGNETIC STUDIES

The previous study of the magnetic properties of the rocks dredged from the Minami–Hiosi submarine volcano using a MA-21 astatic magnetometer showed that the unaltered varieties of basalt and slag were the most magnetic. These data were applied for interpretation of the results of a hydromagnetic survey performed in the 5th voyage of R/V "Vulkanolog" and allowed us to conclude that an intense magnetic anomaly reaching 3000 nT resulted from the rocks of basaltic composition which compose the lava plug [10].

To obtain the full information on the petromagnetic properties of the dredged rocks, which is necessary for interpretation of the materials of the magnetic survey, as well as for study of the nature of magnetism, in this study, we performed the complex petromagnetic investigation of 13 samples obtained from the Minami–Hiosi submarine volcano using the modern methodologies for the first time.

The magnetic parameters were determined by the magnetic hysteresis curves (Fig. 6) with correction for the value of the paramagnetic background (Figs. 7a, 8a, 9a, and 10a).

Our petromagnetic studies showed that most of the samples studied had high values of Jn (~1.1–5.8 A/m) and the Koenigsberger factor Qn (3–22), except for the samples of dolerite (B-5-13-10/2), tuff (B-5-13-13), and slag (B-5-13-sh) (Table 4). The samples are magnetically isotropic with the degree of magnetic anisotropy P' reaching 1.026. Step isothermal magnetization of the rock samples in the constant magnetic field is typical of low-coercivity magnetic minerals: the samples obtain >90% of magnetization in the field of 0.2 T (Figs. 7c, 8c, 9c, and 10c).

According to the dependence of magnetic susceptibility on temperature $k$(T), the curves of the thermomagnetic analysis may be divided into five groups, although such division is arbitrary to some extent (Figs. 7d, 8d, 9d, and 10d).

Group I includes Samples B-5-13-9, B-5-13-10/2, and B-5-13-12/3. The magnetization of the samples of basalt (dolerite) is controlled by the concentration of the low-coercivity magnetic minerals (Bcr = 22–42 mT) with low degree of oxidation ($B_{0.5}$ = 19–36 mT) (Table 4). The curves of thermomagnetic analysis contain two Currier points corresponding to titanomagnetite ($T_c$ ~ 480–490°C) and magnetite ($T_c$ ~ 580°C) (Fig. 7d). The curve of cooling is below the curve of heating, which most likely provides evidence for the transition of magnetite to poorly magnetic hematite during heating up to 700°C [6]. The bulk concentration C of the grains ranges within 0.2–1.4% (Table 4). The structure of the magnetic grains is pseudo-single-domain (PSD).

According to the behavior of the curves of thermomagnetic analysis, group I may include dolerite (Sample B-5-13-9/1) as well, because it contains two ferromagnetic phases: titanomagnetite with the composition close to that of magnetite ($T_c$ ~ 560°C) and hematite ($T_c$ ~ 675°C). The presence of hematite is also evident from the high degree of oxidation ($B_{0.5}$ = 83 mT) and relatively high value of Bcr = 53–55 mT. The curve of cooling upon thermomagnetic analysis is slightly lower and irreversible, which results from the formation of poorly magnetic hematite from magnetite during cooling to 700°C on air. The high magnetization of the dolerite sample (Jn = 2 A/m) is explained by the high concentration of PSD magnetite grains (Table 4).

Group II includes Samples B-5-13-6 and B-5-13-9/2. The high magnetization (Jn = 4–6 A/m) of the dolerite samples results from the high concentration (C ~ 0.7%) of the low-coercivity magnetic minerals (Bcr ~ 22–45 mT) with the low degree of oxidation ($B_{0.5}$ ~ 7–11 T) (Table 4). The curves of thermomagnetic analysis contain three Currier points corresponding to titanomagnetite with Currier points in the ranges of 270–340°C and ~450–550°C and magnetite (~580°C) (Fig. 8d). The structure of the grains is PSD (Table 4).

The crystallochemical formula calculated for the titanomagnetite from Sample B-5-13-6 shows that the concentration of Ti is 0.38 f.u., which corresponds to the calculated Currier point at ~300°C matching with the one experimentally obtained by the TMA method.

According to the curve of thermomagnetic analysis, group II could include dolerite (Sample B-5-13-23). This sample contains three ferromagnetic phases, as well: titanomagnetite ($T_c$ ~ 310°C), titanomagnetite with the composition close to that of magnetite (Tc ~ 550°C), and hematite ($T_c$ ~ 675°C). The curve of cool-

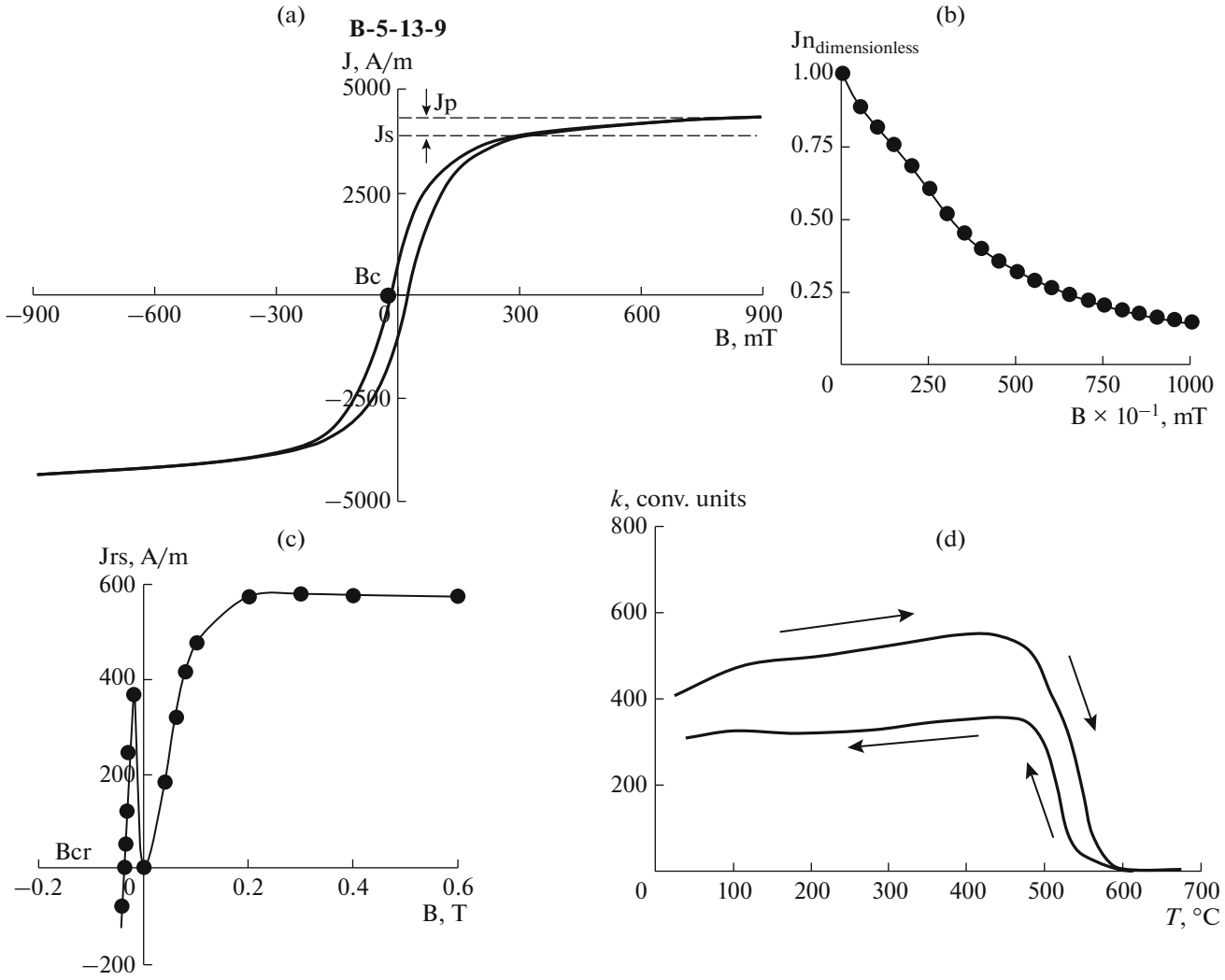


**Fig. 7.** Example of curves of petromagnetic studies for samples of Group I. Magnetic hysteresis (a), result of demagnetization by the alternating magnetic field (b), curve of saturation remanent magnetization of the sample in the constant magnetic field (c), thermomagnetic analysis (d).

ing is slighTy lower and irreversible, which is explained by the formation of poorly magnetic hematite from the magnetite.

The concentration of Ti (0.36 f.u.) in the calculated crystallochemical formula corresponds to the calculated Currier point at ~310°C, which matches with that obtained experimentally by the TMA method.

Group III includes Samples B-5-13-12/1, B-5-13-12/2, and B-5-13-12/4. The relatively high magnetization (Jn ~ 1–4 A/m) of the dolerite samples results from the high concentration (C ~1.5%) of low-coercivity magnetic minerals (Bcr = 14–39 mT) of the PSD structure (Table 4). The thermomagnetic curves of the samples contain two ferromagnetic phases with the Currie points at ~60–100°C and ~580°C (Fig. 9d). The curve of cooling is slighTy lower than the curve of heating, and the curves are irreversible. The phase at ~580°C is stable and occurs both on the curve of heating and on the curve of cooling, which provides evidence for magnetite persistent to heating. After sample heating, the Currier point on the curves of low-temperature phase cooling becomes not so clear or disappears completely, which results from decomposition of the starting magnetite upon heating up to 700°C in air. Thus, the major carriers of magnetization in the samples studied are the grains of magnetite, as well as titanomagnetite with a high concentration of titanium (X = 0.65–0.71) persistent to heating.

Calculation of the crystallochemical formula of the titanomagnetite from the chemical composition shows that the content of Ti in the mineral is 0.59 f.u., which corresponds to the calculated Currier point at ~140°C.

Group IV includes tuff (Samples B-5-13-13 and B-5-13-26/1). Magnetization of the tuff results from the low concentration of magnetic minerals (C ~0.1%) with the Currier points at ~290–320°C, ~460–520°C,

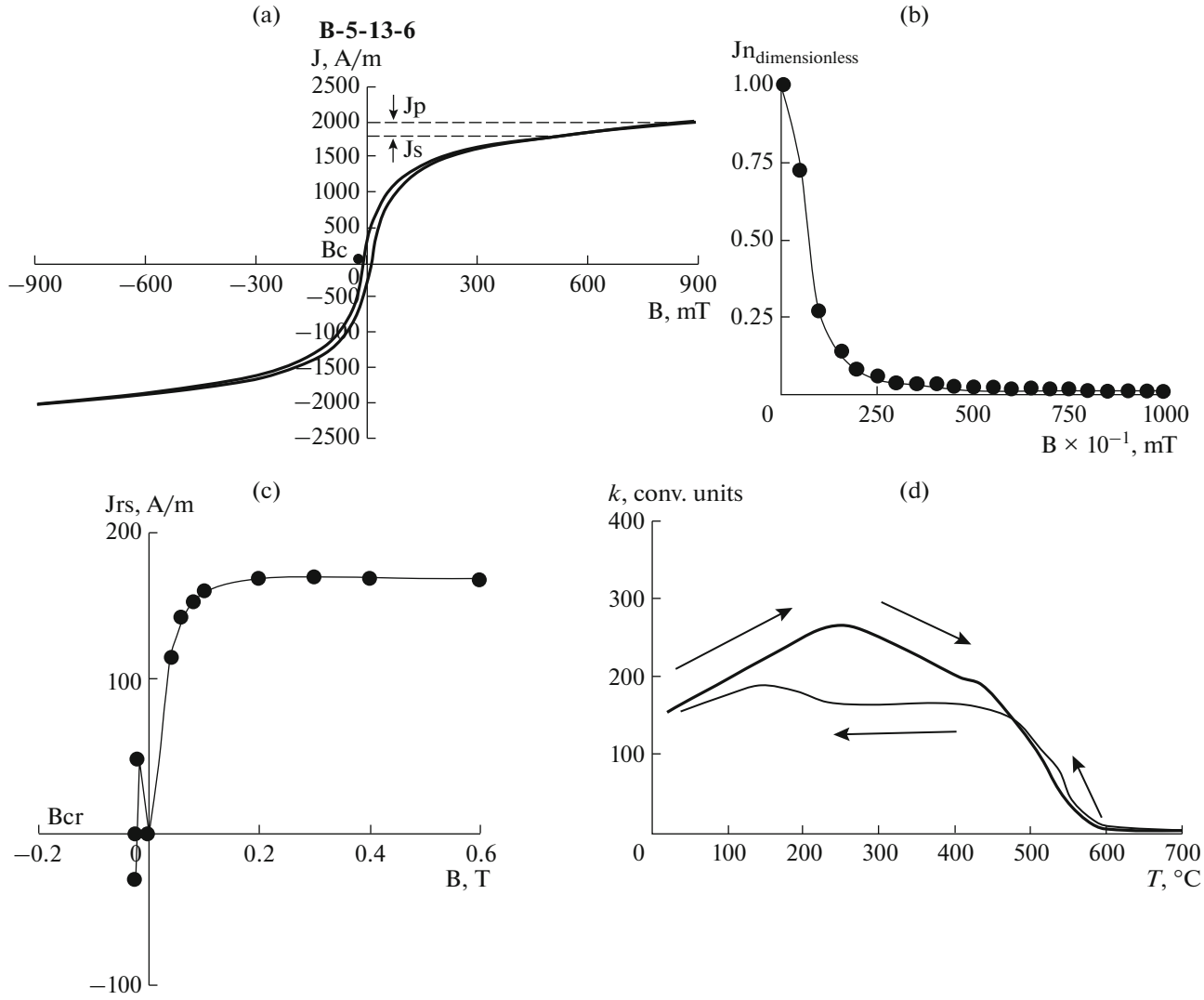


**Fig. 8.** Example of curves of petromagnetic studies for samples of Group II. Magnetic hysteresis (a), result of demagnetization by the alternating magnetic field (b), curve of saturation remanent magnetization of the sample in the constant magnetic field (c), thermomagnetic analysis (d).

~580°C, and ~650–675°C (Fig. 10d). The curve of cooling is much higher and does not contain the Currier point at Tc ~ 290–320°C because heating of the samples resulted in decomposition of the titanomagnetite with the formation of magnetite. The presence of hematite in the composition of the tuff is supported by the rather high values of $B_{0.5}$ ~ 49–79 mT and Bcr ~ 60–61 mT (B-5-13-26/1) (Table 4).

Study of thin sections under the microscope shows a high content of organic material, which explains the high paramagnetic contribution to the curves of magnetic hysteresis (Fig. 10a). The content of the ore minerals is low and they mainly occur in rock fragments. Among the ore minerals are titanomagnetite and hematite, which was formed as a result of olivine decomposition. Thus, the major carriers of magnetization in these samples are titanomagnetite grains with low (X ~ 0.11–0.13), as well as higher (X ~ 0.32–0.39) Ti concentrations.

Group V includes slag (Sample B-5-13-sh), which is characterized by low values of Jn = 5–8 mA/m and the paramagnetic type of the curve of magnetic hysteresis, which cannot be used for estimation of the coercivity parameters. Study of the sample under the microscope shows an absence of ore minerals and a high concentration of organic materials.

## CONCLUSIONS

In spite of the significant volume of geological and geophysical studies previously performed for the Minami–Khiosi submarine volcano, the complex mineralogical and petromagnetic studies of the rocks com-

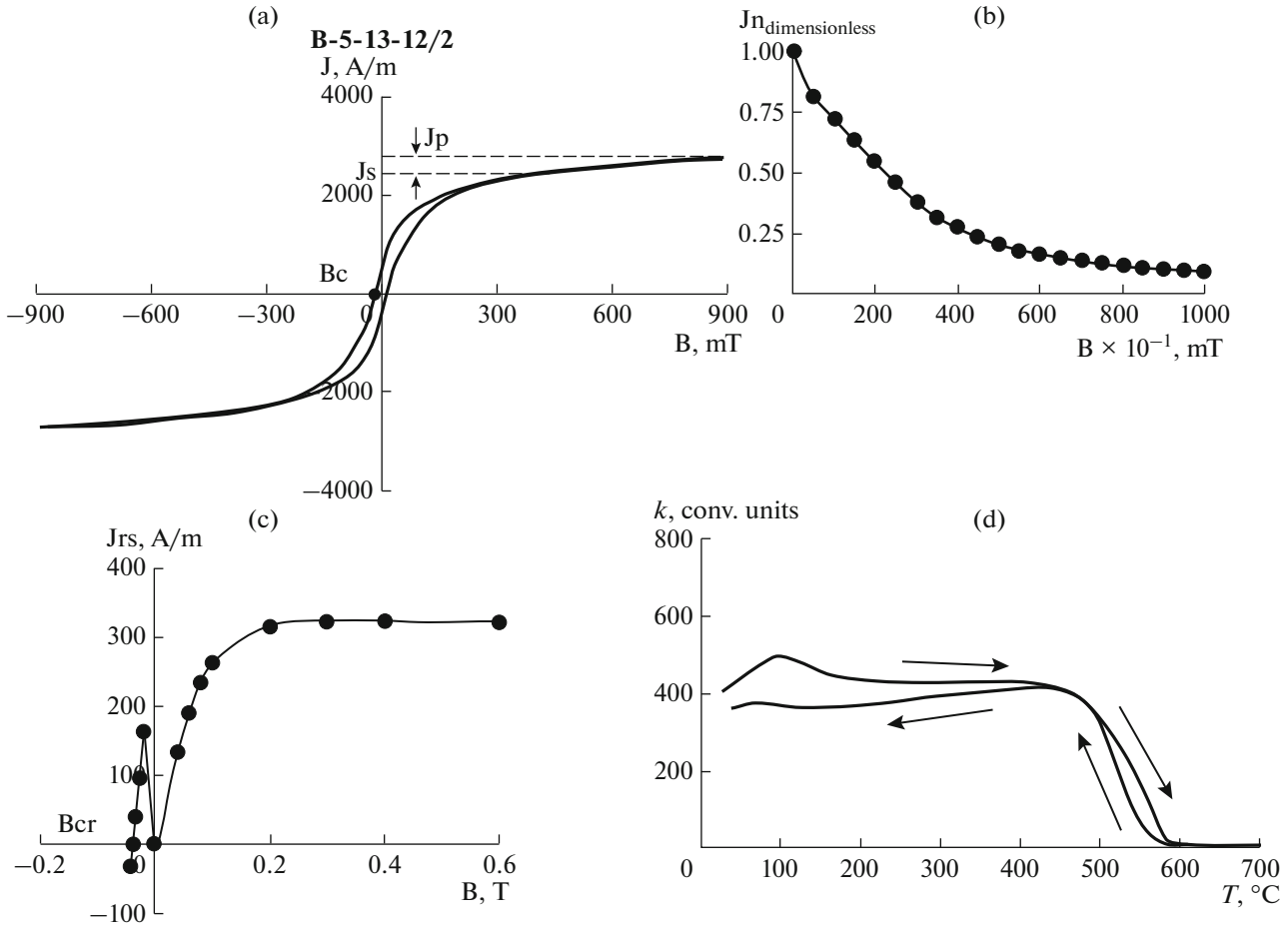


**Fig. 9.** Example of curves of petromagnetic studies for samples of Group III. Magnetic hysteresis (a), result of demagnetization by the alternating magnetic field (b), curve of saturation remanent magnetization of the sample in the constant magnetic field (c), thermomagnetic analysis (d).

posing the volcanic edifice are carried out for the first time in the present work.

The volcanic edifice is composed of basalt with various textural and structural characteristics, more silica-rich volcanic rocks (alkali trachyandesite-basalt and trachyte), as well as their slags. Study of the mineral and chemical composition of the rocks sampled on the Minami–Khiosi Volcano shows that they are alkaline. Our studies and the published data show that the Minami–Khiosi submarine volcano is part of the group of alkaline volcanoes distinguished within the Idzu–Bonin and Mariana island arcs.

It is established that most of the samples studied have high values of Jn ~ 1–6 A/m and Koenigsberger factor Qn ~ 3–22. The samples are magnetically isotropic with the degree of magnetic isotropy P' reaching 1.026. Similarly to other island-arc Late Cenozoic volcanoes in the western part of the Pacific Ocean [2, 3, 7, 8, 12–15], the samples studied are strongly differentiated by the values of Jn and *k*. The major carriers of magnetization are the low-coercivity magnetic minerals (titanomagnetite and magnetite) of the pseudo-single-domain structure, as well as the high-coercivity minerals (hematite). The high values of Jn in the rock samples studied result from the pseudo-single-domain structure of the titanomagnetite grains, whereas the high values of *k* are explained by the high concentration of ferromagnetic grains.

Complex interpretation of the data obtained (Table 4) shows that neither the texture of the rock, nor the size of the ferromagnetic minerals, nor the proportions between the titanomagnetite and ilmenite influence the magnetic behavior of the rocks upon heating. According to the concentration of Ti in the titanomagnetite, five groups of rocks are distinguished, which is reflected in the results of thermomagnetic analysis by the dependence of magnetic susceptibility on temperature $k(T)$. Group I is characterized by the Currier points corresponding to titanomagnetite ($T_c$ ~ 480–490°C), magnetite (T ~ 580°C), and rarely hematite ($T_c$ ~ 675°C) on the curves of thermomagnetic analysis. In this group, the concentration of Ti in the titanomagnetite is the lowest (from 2.8, on average 6.5 wt %, or 0.27 f.u. Ti per ele-

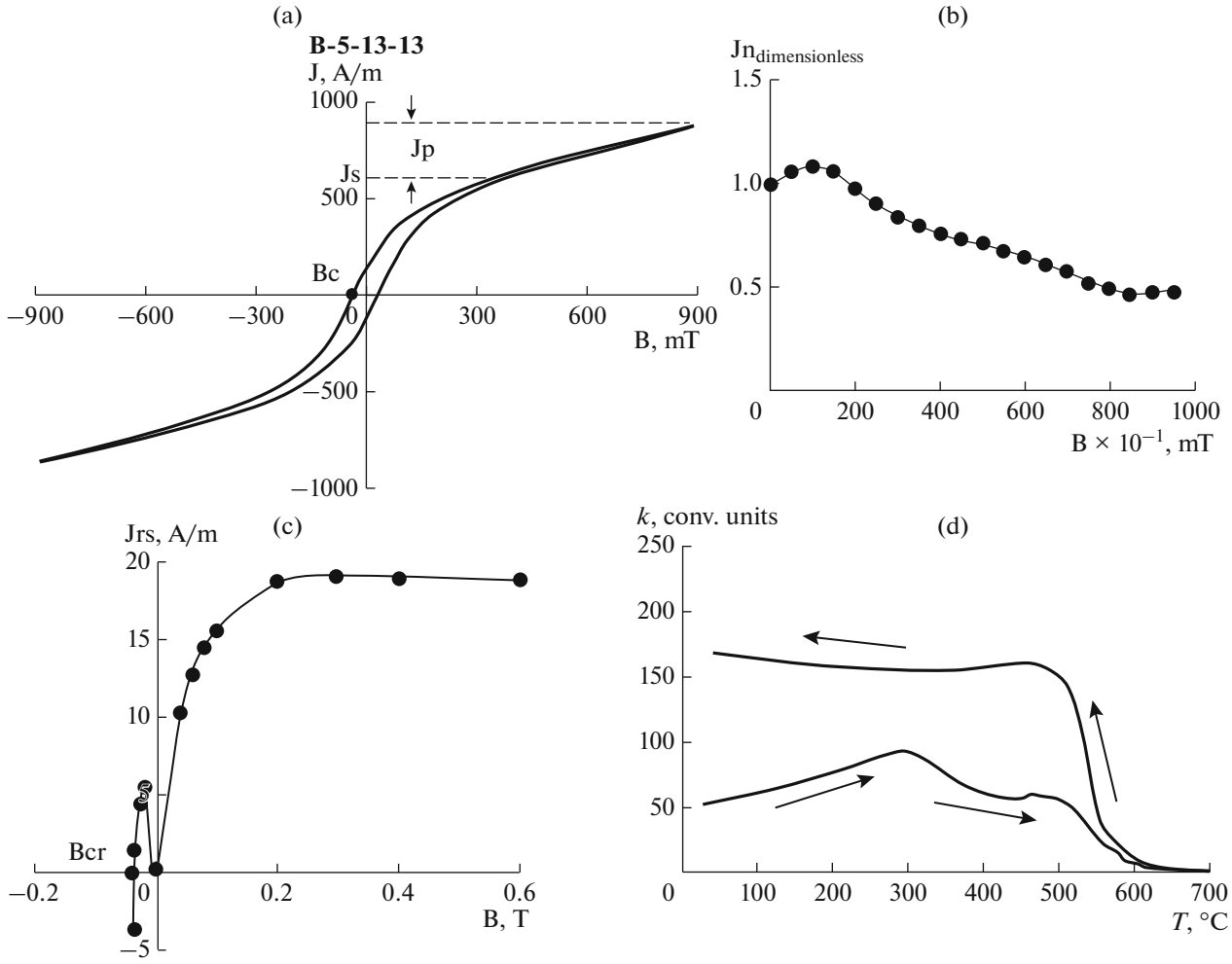


**Fig. 10.** Example of curves of petromagnetic studies for samples of Group IV. Magnetic hysteresis (a), result of demagnetization by the alternating magnetic field (b), curve of saturation remanent magnetization of the sample in the constant magnetic field (c), thermomagnetic analysis (d).

mentary cell). The presence of the Currier point of hematite is explained by the primary occurrence of some contents of this mineral in the rocks. Hematite is incorporated in the composition of iddingsite that is the late aggregate of Fe oxides, hydroxides, and layered silicates replacing olivine. Some portions of iddingsite occur in all samples.

Group II includes the samples with the Currier points corresponding to titanomagnetite (270–340°C and ~450–550°C) and magnetite (~580°C) on the curves of thermomagnetic analysis. This group is characterized by a much higher content of Ti in the titanomagnetite (from 7 to 10, on average 8–9 wt %, or 0.36–0.38 f.u. per elementary cell of titanomagnetite).

Group III includes the samples with thermomagnetic curves containing two ferromagnetic points with the Currier points at ~60–100°C and ~580°C corresponding to both titanomagnetite with the high Ti concentration and magnetite grains persistent to heating. In fact, these samples are characterized by the highest Ti concentration in the titanomagnetite (14–15 wt % or 0.59 f.u. Ti per elementary cell of titanomagnetite).

Group IV was not analyzed on a microprobe because the samples were collected from tuff, which is a mixture of rocks from groups I, II, and III.

The rock of group V is represented by slag, in which Fe-bearing minerals are absent.

As a result of the studies performed, we obtained additional information on the textural, petrographic, and mineralogical peculiarities and petromagnetic properties of the rocks composing the edifices of the Late Cenozoic island-arc submarine volcanoes in the western part of the Pacific Ocean. The data obtained may be applied later in various aspects by researchers studying the Pacific transitional zone.

**Table 4.** Petromagnetic characteristics of rock samples dredged from the Minami–Khiosi submarine volcano

| No. | Sample no. | Jn, A/m | $\chi \times 10^{-3}$, CI | Qn | P' | $B_{0.5}$, mT | Jrs, A/m | Js, A/m | Jrs/Js | Bcr, mT | Bc, mT | Bcr Bc | Structure | C, % |
|---|---|---|---|---|---|---|---|---|---|---|---|---|---|---|
| 1-1 | B-5-13-6-1 | 5.251 | 14.63 | 9.02 | 1.022 | – | 358.2 | 2281.5 | 0.2 | 23.2 | 10.7 | 2.2 | PSD | 0.7 |
| 1-2 | B-5-13-6-2 | 5.884 | 12.46 | 11.87 | 1.017 | 7.3 | 329.3 | | | 21.9 | | | | |
| 2-1 | B-5-13-9-1 | 3.067 | 24.29 | 3.17 | 1.008 | – | 908.0 | 4035.6 | 0.2 | 42.1 | 20.5 | 2.1 | PSD | 1.1 |
| 2-2 | B-5-13-9-2 | 3.261 | 23.84 | 3.44 | 1.008 | 31.2 | 874.1 | | | 42.2 | | | | |
| 3-1 | B-5-13-9/1-1 | 2.163 | 5.61 | 9.69 | 1.020 | – | 337.40 | 1254.3 | 0.3 | 53.1 | 31.0 | 1.7 | PSD | – |
| 3-2 | B-5-13-9/1-2 | 2.242 | 5.165 | 10.91 | 1.020 | 83 | 300.5 | | | 54.8 | | | | |
| 4-1 | B-5-13-9/2-1 | 4.036 | 21.06 | 4.82 | 1.010 | – | 657.5 | 3354.6 | 0.2 | 45.1 | 17.5 | 2.6 | PSD | – |
| 4-2 | B-5-13-9/2-2 | 5.019 | 23.52 | 5.36 | 1.016 | 10.5 | 768.6 | | | 45.0 | | | | |
| 5-1 | B-5-13-10/2-1 | 0.265 | – | – | – | – | | | | | | | | |
| 5-2 | B-5-13-10/2-2 | 0.226 | 4.93 | 1.35 | 1.018 | 19 | 81.4 | 733.3 | 0.1 | 22.3 | 9.9 | 2.3 | PSD | 0.2 |
| 6-1 | B-5-13-12/1-1 | 2.974 | 21.57 | 3.46 | 1.005 | – | 550.0 | 2864.6 | 0.2 | 36.9 | 12.7 | 2.9 | PSD | 1.5 |
| 6-2 | B-5-13-12/1-2 | 2.063 | 19.26 | 2.69 | 1.005 | 30.5 | 511.3 | | | 38 | | | | |
| 7-1 | B-5-13-12/2-1 | 2.949 | 17.66 | 4.20 | 1.008 | – | 550.1 | 2450.3 | 0.2 | 38.7 | 14.7 | 2.6 | PSD | – |
| 7-2 | B-5-13-12/2-2 | 3.877 | 20.94 | 4.65 | 1.007 | 22.5 | 643.2 | | | 38.2 | | | | |
| 8-1 | B-5-13-12/3-1 | 4.897 | 35.99 | 3.42 | 1.011 | – | 1097 | 6060.8 | 0.2 | 30.3 | 15.0 | 2.0 | PSD | 1.4 |
| 8-2 | B-5-13-12/3-2 | 4.358 | 34.78 | 3.15 | 1.008 | 35.5 | 1108 | | | 30.3 | | | | |
| 9-1 | B-5-13-12/4-1 | 1.453 | 16.86 | 2.17 | 1.007 | – | 181.4 | 1511.7 | 0.1 | 13.5 | 4.9 | 2.8 | PSD | |
| 9-2 | B-5-13-12/4-2 | 2.361 | 24.35 | 2.44 | 1.008 | 11.7 | 236.3 | | | 16.2 | | | | |
| 10-1 | B-5-13-13-1 | 0.035 | 2.43 | 0.36 | 1.005 | – | 41.0 | 194.2 | 0.2 | 37.8 | 30.1 | 1.3 | ? | 0.1 |
| 10-2 | B-5-13-13-2 | 0.053 | 2.62 | 0.51 | 1.009 | 78.5 | 37.7 | | | 35.7 | | | | |
| 11-1 | B-5-13-23-1 | 2.854 | 3.36 | 21.34 | 1.005 | – | 165.5 | 1047.5 | 0.2 | 62.9 | 14.8 | 4.3 | ? | 0.3 |
| 11-2 | B-5-13-23-2 | 2.264 | 2.51 | 22.65 | 1.005 | 33.0 | 122.8 | | | 62.9 | | | | |
| 12-1 | B-5-13-26/1-1 | 1.139 | 2.97 | 9.64 | 1.008 | – | 94.3 | 392.9 | 0.2 | 61.2 | 23.7 | 2.6 | PSD | – |
| 12-2 | B-5-13-26/1-2 | 1.308 | 3.68 | 8.93 | 1.006 | 49 | 104.8 | | | 59.8 | | | | |
| 13-1 | B-5-13-sh-1 | 0.008 | 0.27 | 0.74 | 1.008 | – | 1.4 | – | – | 91.6 | – | – | – | – |
| 13-2 | B-5-13-sh-2 | 0.005 | 0.37 | 0.34 | 1.026 | 71 | 1.5 | | | 90.7 | | | | |

Jn, natural remanent magnetization; $\chi$, magnetic susceptibility; Qn, Koenigsberger factor; P', degree of magnetic susceptibility anisotropy; $B_{0.5}$, median field; Jrs, saturation remanent magnetization; Js, saturation magnetization; Bcr, remanent coercivity force; Bc, coercivity force; C, bulk ferromagnetic concentration; PSD, pseudo-single-domain grains; "–", characteristic was not analyzed; "?", characteristic was not determined.

## ACKNOWLEDGMENTS

This study was supported by the Russian Foundation for Basic Research (project no. 15-05-02955-a).

## REFERENCES

1. V. A. Aprodov, *Volcanoes* (Mysl', Moscow, 1982) [in Russian].
2. Yu. I. Blokh, V. I. Bondarenko, A. S. Dolgal', P. N. Novikova, O. V. Pilipenko, V. A. Rashidov, and A. A. Trusov, "Application of modern computer technologies for study of submarine volcanic center in the vicinity of the southwestern termination of Simushir Island (Kuril island arc)," Vestn. KRAUNTs. Nauki O Zemle, No. 24, 27–40 (2014).
3. Yu. I. Blokh, V. I. Bondarenko, A. S. Dolgal', P. N. Novikova, V. V. Petrova, O. V. Pilipenko, V. A. Rashidov, and A. A. Trusov, "Complex studies of island arc submarine volcanoes of the northwestern Pacific Ocean, in *4th International Scientific–Practical Conference on Marine Studies and Education: MARESEDU-2015, Moscow, Russia, 2015,* (Mosk. Gos. Univ., Moscow, 2015), pp. 63–65 [in Russian].
4. A. P. Gorshkov, V. A. Abramov, E. A. Sapozhnikov, N. I. Seliverstov, and V. A. Rashidov, "Geological structure of Esmeral'da submarine volcano," Vulkanol. Seismol., No. 4, 65–78 (1980).
5. *International Geological–Geophysical Atlas of the Pacific Ocean*, ed. by G. B. Udintsev (MOK (YuNESKO), RAN, FGUP PKO "Kartografiya", GUNiO, Moscow–St. Petersburg, 2003) [in Russian].
6. D. M. Pecherskii and A. N. Didenko, *Paleoasian Ocean: Petromagnetic and Paleomagnetic Information on its Lithisphere* (OIFZ RAN, Moscow, 1995) [in Russian].
7. O. V. Pilipenko, V. A. Rashidov, and V. V. Petrova, "Petromagnetic studies of the rocks of submarine volcanoes of the Kuril Island Arc," *Paleomagnetism and Magnetism of Rocks. Proceedings of International School–Seminar on Problems of Paleomagnetism and Magnetism of Rocks, St. Petersburg, Russia, 2014* (SOLO, St. Petersburg, 2014), pp. 133–140 [in Russian].
8. O. V. Pilipenko and V. A. Rashidov, "New data on the petromagnetic properties of rocks that compose the submarine volcanoes of the Kuril Island arc," in *Proceedings of 3rd School–Conference "Gordin Readings," Moscow, Russia, 2015* (IFZ RAN, Moscow, 2015), pp. 17–22 [in Russian].
9. V. A. Rashidov, A. P. Gorshkov, and A. N. Ivanenko, "Magnetic studies above the submarine Esmeral'da and Sofu volcanoes," in *Electromagnetic Study of Deep Structure of the Earth's Crust and Upper ManTe in the Sea and Ocean Areas* (IZMIRAN, Moscow, 1981), pp. 213–218 [in Russian].
10. V. A. Rashidov, "Geomagnetic studies of the Minami–Hiyoshi and Fukudzin volcanoes (Mariana Island Arc)," Vulkanol. Seismol., No. 5, 55–64 (2001).
11. V. A. Rashidov, "Geophysical fields of active island-arc submarine volcanoes: measurements and interpretation," Ural. Geofiz. Vesti, No. **8**, 29–35 (2005).
12. V. A. Rashidov, O. V. Pilipenko, and V. M. Ladygin, "A comparative analysis of magnetic properties in rocks: five active submarine volcanoes in the Western Pacific," J. Volcanol. Seismol. **8** (3), 168–182 (2014).
13. V. A. Rashidov, O. V. Pilipenko, and V. V. Petrova, "Petromagnetic and microprobe studies of rocks in the Sofu underwater volcanic cluster, Izu–Bonin Island Arc, Pacific Ocean," J. Volcanol. Seismol. **9** (3), 182–196 (2015).
14. V. A. Rashidov, O. V. Pilipenko, and V. V. Petrova, "Geological–geophysical studies of Minami–Hiyoshi submarine volcano, Mariana Island Arc," in *Sea and Ocean Geology: Proceedings of 21st International Conference (School) on Marine Geology, Moscow, Russia, 2015* (GEOS, Moscow, 2015), Vol. 5, pp. 237–241 [in Russian].
15. V. A. Rashidov, O. V. Pilipenko, and V. V. Petrova, "Rock magnetic and petrographical–mineralogical studies of the dredged rocks from the submarine volcanoes of the Sea-of-Okhotsk slope within the northern part of the Kuril Island Arc," Izv. Phys. Solid Earth, **52** (4), 550–571 (2016).
16. Sh. H. Bloomer, R. J. Stern, E. Fisk, and C. H. Geschwind, "Shoshonitic volcanism in the northern Mariana Arc. 1. Mineralogic and major and trace element characteristics," J. Geophys. Res. **94** (B4), 4469–4496 (1989).
17. Sh. H. Bloomer, R. J. Stern, and N. Chr. Smoot, "Physical volcanology of the submarine Mariana and volcano arcs," Bull. Volcanol. **59** (3), 210–224 (1989).
18. R. Day, M. Fuller, and V. A. Schmidt, "Hysteresis properties of titanomagnetites: grain-size and compositional dependence," Phys. Earth Planet. Inter. **13**, 260–267 (1977).
19. D. J. Dunlop, "Theory and application of the day plot (Mrs/Ms versus Hcr/Hc). 1. Theoretical curves and tests using titanomagnetite data," J. Geophys. Res. **107** (B3) (2002). doi 10.1029/2001JB000486
20. R. W. Embley, E. T. Baker, W. W. Chadwick, J. E. Lupton, J. A. Resing, G. J. Massoth, and K. Nakamura, "Explorations of Mariana arc volcanoes reveal new hydrothermal systems," EOS **85** (4), 37–40 (2004).
21. T. L. Wright and D. L. Peck, "Magnetic properties and oxidation of iron-titanium oxide minerals in Alae and Makaopuhi lava lakes, Hawaii," J. Geophys. Res. **74**, 5277–5294 (1969).
22. T. Yamazaki, "Gravity anomalies over the Izu–Oga–Sawara (Bonin) and Mariana arcs," Bull. Geol. Serv. Japan **42** (12), 687–701 (1991).
23. T. Ishihara, "A new leveling method without the direct use of crossover data and its application in marine magnetic surveys: weighted spatial averaging and temporal filtering," Earth Planet. Sp. **67** (1), 11 (2015).
24. D. Lattard, R. Engelmann, A. Kontny, and U. Sauerzapf, "Curie temperatures of synthetic titanomagnetites in the Fe–Ti–O systems. Reassessment of some methodological and crystal chemical effects," J. Geophys. Res. **111** (12), 28 (2006).
25. P.-N. Lin, R. J. Stern, and Sh. H. Bloomer, "Shoshonitic volcanism in the northern Mariana Arc. 2. Large-ion lithophile and rare earth element abundances: evidence for the source of incompatible element enrich-

ments in intraoceanic arcs," J. Geophys. Res. **94** (B4), 4497–4514 (1989).

26. P.-N. Lin, R. J. Stern, J. Morris, and Sh. H. Bloomer, "Nd- and Sr isotopic compositions of lavas from the Northern Mariana and Southern volcano arcs: implications for the origin of island arc melts," Contrib. Mineral. Petrol. **105**, 381–392 (1990).
27. F. Martinez, P. Fryer, N. A. Baker, and T. Yamazaki, "Evolution of backarc rifting: Mariana Trough, 20°–24° N," J. Geophys. Res. **100** (B3), 3807–3827 (1995).
28. J. K. Meen, R. J. Stern, and Sh. H. Bloomer, "Evidence for magma mixing in the Mariana arc system," The Island Arc **7**, 443–459 (1998).
29. A. Nishizawa and N. Sasahara, "Ocean bottom seismographic observation at Minami–Hiyoshi Seamount at the northern end of the Mariana Arc," Rept. Hydrograph. Oceanograph. Res., No. 39, 3–19 (2003).
30. Y. Otani, M. Tsuchide, A. Shibata, Sh. Kato, Y. Iwabuchi, "The list of volcanoes and their activities records in the adjacent seas of Japan. 3rd Ed," Rept. Hydrograph. Oceanograph. Res., No. 40, 1–62 (2004).
31. J. A. Pearce, R. J. Stern, Sh. H. Bloomer, and P. Fryer, "Geochemical mapping of the Mariana arc–basin system: implications for the nature and distribution of subduction components," Geochem. Geophys. Geosyst **6** (7), Q07006 (2005).
32. E. Petrovsky and A. Kapicka, "On determination of the Curie point from thermomagnetic curves," J. Geophys. Res. **111**, 27 (2006).
33. A. Shibata, "Description of volcanic eruption," Bull. Volcan. Erup., no. 32, 36 (1995).
34. L. Siebert and P. Kimberly, *Volcanoes of the World* (Univ. California Press, Berkeley, 2010).
35. N. S. Smoot, "The growth rate of submarine volcanoes on the South Honshu and East Mariana ridges," J. Volcanol. Geotherm. Res. **35**, 1–15 (1988).
36. N. S. Smoot, "Discussion "The growth rate of submarine volcanoes on the South Honshu and East Mariana ridges". Reply," J. Volcanol. Geotherm. Res. **45**, 341–345 (1991).
37. C.-H. Sun, R. J. Stern, and J-I. Kimura, "Fukutoku–Oka–No–Ba volcano: a new perspective on the alkalic volcano province in the Izu-Mariana Arc," The Island Arc **7**, 432–442 (1998).
38. C.-H. Sun, R. J. Stern, J. Naka, I. Sakamoto, M. Arima, "Geological and Geochemical Studies with Dolphin 3 K on North Hiyoshi Seamount, Izu–Bonin–Mariana, AMSTECd," Deep Sea Res. **14**, 139–156 (1999).
39. C.-H. Sun and R. J. Stern, "Genesis of Mariana shoshonites: contribution of the subduction component," J. Geophys. Res. **106** (B1), 589–608 (2001).
40. F. Murakami, "Magnetic anomalies over the Izu-Ogasawara (Bonin) Arc, Mariana Arc and Mariana Trough," Bull. Geol. Serv. Japan **42** (12), 655–686 (1991).
41. E. Murakami and E. Saito, "Mode of seafloor spreading in the northern Mariana Trough," Tectonophysics **221**, 207–222 (1993).
42. F. Murakami, "Asymmetric Rifting of the northern Mariana Trough," The Island Arc **7**, 460–470 (1998).
43. M. Yasa, F. Murakami, E. Saito, and K. Watanabe, "Submarine topography of seamounts on the volcanic front of the Izu–Ogas–Avara (Bonin) Arc," Bull. Geol. Serv. Japan **12** (12), 703–743 (1991).

*Recommended for publishing by A.N. Didenko*

*Translated by A. Bobrov*